IEEE Access
Multidisciplinary | Rapid Review | Open Access Journal

Received September 2, 2019, accepted September 19, 2019, date of publication September 30, 2019,
date of current version October 10, 2019.

Digital Object Identifier 10.1109/ACCESS.2019.2944479

An Optimal Torque Distribution Control Strategy for Four-Wheel Independent Drive Electric Vehicles Considering Energy Economy

JIANJUN HU[1,2], JUNLONG TAO[2], FENG XIAO[2], XIYUAN NIU[3], AND CHUNYUN FU[1,2]

[1]The State Key Laboratory of Mechanical Transmission, Chongqing University, Chongqing 400044, China
[2]School of Automotive Engineering, Chongqing University, Chongqing 400044, China
[3]GAC Research and Devlopment Center, Chassis Department, Guangzhou 510000, China

Corresponding author: Jianjun Hu (hujianjun@cqu.edu.cn)

This work was supported in part by the National Key Research and Development Program of China under Grant 2018YFB0106104, and in part by the Chongqing Key Research and Development Program under Grant cstc2018jszx-cyztzx0047.

ABSTRACT To further improve the energy economy of a four-wheel independent drive electric vehicle (FWIDEV) in the process of vehicle stability control, in this paper, the influence of different wheel torque distributions on vehicle stability and energy economy during vehicle steering is analyzed in depth. Then the wheel torque distribution scheme when the vehicle steering is established. Combined with the economic-based torque distribution strategy applied in the straight running condition, an optimal wheel torque distribution strategy is proposed for FWIDEV to adapt different driving conditions. And the controller designed in this paper adopts hierarchical control structure. The upper controller calculate the corrective yaw moment based on the sliding mode control. The lower controller implements wheel torque distribution according to the proposed strategy. Finally, the simulation results under different driving scenarios indicate that the proposed control strategy can achieve the same effect as the conventional control strategy in terms of vehicle stability, but the energy economy is improved by about 2.4%.

INDEX TERMS Electric vehicles, stability control, optimal torque distribution, energy economy.

I. INTRODUCTION

Electric vehicles are considered to be an effective way to solve problems such as environmental pollution and energy shortage due to their higher efficiency, low noise and nearly zero emissions [1], [2]. From the view point of control engineering, Four-wheel independent drive electric vehicles (FWIDEVs) have much attractive potential for its four in-wheel motors can be controlled independently., which make FWIDEV's handling and stability control become a research hotspot in recent years [3]–[5].

In order to keep the vehicle stable and safety under emergency situations, a variety of chassis control systems have been developed such as four-wheel steering (4WS), active front steering (AFS), direct yaw-moment control (DYC) and so on. 4WS adjusts the steering angle of the rear wheel according to the error between the actual yaw rate of the vehicle and the reference value to change the lateral force on the rear wheel [6], [7]. And AFS is to add a certain additional angle to the front wheel to produce the lateral force of the front axle [8], [9]. When the lateral acceleration of the vehicle is relatively small, the lateral force has a linear relationship with the wheel side angle. At this time, both 4WS and AFS have relatively ideal control effects. While, when the lateral acceleration is large, the lateral force tends to be saturated, which will make the 4WS and AFS will lose their control ability. DYC is a method to improve vehicle handling stability by using the difference of longitudinal forces of the wheel to generate yaw moment [10], [11], and it has been proven to maintain a better performance when the tire is close to the adhesion limit [12]. Most stability controllers use hierarchical control structures. The literature [13], taking the tire slip rate as the design variable, determines the required yaw moment by controlling the tire slip rate to its ideal value, thereby adjusting the longitudinal force of each wheel to achieve DYC. Sun *et al.* [14] taken the yaw rate as the control variable and constructed a robust control methodology based on the front and rear steering angle. Tian *et al.* [15] designed the

The associate editor coordinating the review of this manuscript and approving it for publication was Chao Yang.

phase plane by using the side slip angle and its derivative, and designed the DYC by controlling the actual state of the vehicle in the stable area as the control target. In fact, the yaw rate and the side slip angle of the vehicle are closely related to the stability of the vehicle. Controlling only one of the variables is not suitable for achieving vehicle stability. Therefore, many controllers use both the yaw rate and the side slip angle as control variables, and achieve better performance than that use a single control variable [16], [17]. For the calculation of the desired yaw moment, J.HAN uses the LQR method [18], and other control methods include fuzzy control [19], model predictive control, robustness control, and sliding mode variable structure control [20]–[22]. However, no matter which control method is adopted, the above literature mainly focuses on the research of the upper controller, and the distribution rule of the lower layer torque is relatively simple, which results in poor stability and adaptability of the control system.

On the other hand, in the vehicle stability control, the required yaw moment calculated based on different control variables or by different methods needs to be realized by the motor and the wheel of the execution layer, that is, the wheel torque needs to be distributed. The current research is mainly based on two methods of distribution: one is based on the economical torque distribution method. Wu *et al.* [23] proposed an optimal wheel torque distribution strategy based on the motor loss model. Yamakawa and Watanabe[24] proposed a wheel driving force distribution method to reduce the friction loss of each wheel, thereby improving vehicle economy. Energy recovery is one of the important ways to save energy in electric vehicles. The literature [25] details the current status and development of braking energy recovery. For electric vehicles, the improvement of motor efficiency has more significant economic improvement performance [26], [27]. The main idea is to optimize the torque distribution based on the motor efficiency characteristics, so that the motor operating point is always in the high efficiency area. Although the above research can improve the efficiency of the transmission system, most of them are less concerned with the stability control of the vehicle. Another type of method is a torque distribution strategy based on vehicle stability. Osama proposed a mathematical optimization method that optimizes tire utilization to distribute wheel torque [28]. This method of setting objective function ignores vehicle dynamics. There is a certain limitation in the single use of stability or economic methods for torque distribution, and most of the research focus on the straight driving condition of vehicles, while few researches on the economic improvement in the process of vehicle stability control under steering condition.

In summary, wheel torque distribution is extremely important for FWIDEV stability control. There are many different torque distribution methods under the premise of meeting the stability requirements. However, the research on the influence of different wheel torque distribution forms on vehicle performance is not deep enough. In addition, most wheel torque distribution strategies are less concerned with the difference between the vehicle's steering conditions and the straight running conditions, making the vehicle's control effect in the actual driving process is not good. Therefore, in order to make up for the above deficiencies, this paper optimizes the stability controller, and deeply analyzes the impact of different torque distribution forms on vehicle performance, and improves the vehicle economy in the steering process according to its influence law. On the basis, a wheel torque optimization distribution control strategy suitable for the whole driving conditions of the vehicle is applied, thereby comprehensively improving the economy on the basis of ensuring the stability of the vehicle.

The paper is structured as follows. The control strategy begins with a 8-DOF vehicle model in Section II. In Section III, the sliding mode control algorithm is adopted to design the stability controller. Then, a wheel torque optimal distribution control strategy suitable for different driving conditions is established. Section IV shows the simulation results to evaluate the proposed driving control strategy. Finally, the conclusions are provided in Section V.

II. VEHICLE MODELING

A. 8-DOF VEHICLE MODEL

This paper takes a four-wheel independent drive electric vehicle as the research object, and the vehicle parameters are shown in table 1. The most commonly used nonlinear vehicle models include 7-DOF, 8-DOF and 14-DOF. As to vehicle yaw stability control, the 8-DOF vehicle model is taken in this study for the higher accuracy of vehicle response and avoiding excessive computation load. Based on the Matlab/Simulink, the eight degrees of vehicle model that contains vehicle longitudinal, lateral, roll and yaw motions and the rotational motion of each wheel is built (Fig.1).

where, XOY is the geodetic coordinate system, xoy is the vehicle coordinate system, and $x'o'y'$ is the tire coordinate system.

Applying Newton's second law, the equations of the longitudinal, lateral, roll and yaw motions are obtained:

$$\sum_{i=1}^{4}\left(F_{xi}cos\delta - F_{yi}sin\delta\right) - F_w - F_f - F_i - F_j = m\left(\dot{v_x} - v_y r\right) + m_s h_s \dot{p r} \tag{1}$$

$$\sum_{i=1}^{4}\left(F_{xi}sin\delta + F_{yi}cos\delta\right) = m\left(\dot{v_y} + v_x r\right) + m_s h_s \dot{p} \tag{2}$$

$$\sum_{i=1}^{4} x_i\left(F_{xi}sin\delta + F_{yi}cos\delta\right) - \sum_{i=1}^{4} y_i\left(F_{xi}cos\delta - F_{yi}sin\delta\right) = I_z\dot{r} - I_{xz}\dot{p} \tag{3}$$

$$-K_{\emptyset}\emptyset + m_s g h_s sin\emptyset - C_{\emptyset}p = I_z\dot{p} - I_{xz}\dot{r} - m_s h_s(\dot{v_y} + v_x r) \tag{4}$$

where F_{xi} and F_{yi} represent the longitudinal and lateral tyre forces respectively, F_w, F_f, F_i, and F_j denote the air resistance, rolling resistance, grade resistance and acceleration resistance, respectively. r is the yaw rate, p, $\emptyset$ and δ are the roll rate, roll angle and the front wheel steer angle respectively.

TABLE 1. Vehicle parameters of FWIDEV.

Symbol	Quantity	Value
m	Vehicle total mass	1300 kg
m_s	Sprung mass	1170 kg
l_f	Distance form CG to front axle	1.2 m
l_r	Distance form CG to rear axle	1.3 m
d	Wheel base	1.4 m
h	Mass center height	0.5 m
h_s	Distance	0.4 m
h_{rcf}	Front roll center height	0.1 m
h_{rcr}	Front roll center height	0.13 m
I_x	Roll moment of inertia	700 kg · m^2
I_z	Yaw moment of inertia	2500 kg · m^2
J	Inertia of wheel assembly	2.1 kg · m^2
K_f	Front suspension roll stiffness	25200 Nm/rad
K_r	Rear suspension roll stiffness	19800 Nm/rad
$K_\emptyset$	Roll stiffness	45000 Nm/rad
C_f	Front suspension roll damping	1300 Nms
C_r	Rear suspension roll damping	1300 Nms
$C_\emptyset$	Roll damping	2600 Nms
R	Tire radius	0.316 m

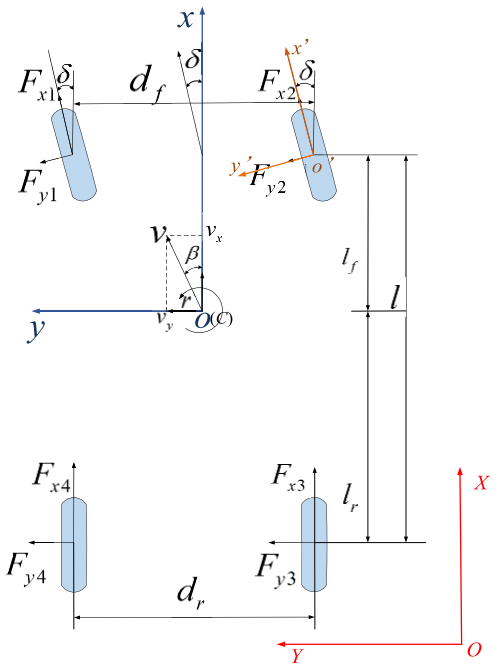

FIGURE 1. The 8-DOF vehicle model.

I_{xz} denotes the product of inertia with respect to the xz plane, v_x and v_y represent the longitudinal velocity and lateral velocity of the vehicle.

Note that the subscript i takes on values 1, 2, 3 and 4, and represents the front left, front right, rear right and rear left wheel respectively, as shown in Figure 1. Besides, when the car is driving, the equation on each tire is that:

$$J\frac{d\omega}{dt} = T - F_x R - F_z \tag{5}$$

where J denotes the rotational inertia of the wheel, ω represents the rotation of the wheel angular velocity. F_z and F_x are the normal reaction force from the ground and the longitudinal force of the tyre, respectively.

B. STEERING SYSTEM MODEL

In order to give consideration to the flexibility and stability of vehicle steering, a steering system with variable steering ratio is established in this paper [29]. The expression is shown in (6).

$$\mathrm{y} = \begin{cases} 10, & 0 < v_x < 30 \\ 0.00139\times (v_x - 30)^2 + 10, & 30 \le v_x < 90 \\ 0.00139 \times (v_x - 150)^2 + 20, & 90 \le v_x < 150 \\ 20, & \text{others} \end{cases} \tag{6}$$

C. TYRE MODEL

As the only connection between the vehicle and the ground, the tyre plays an important role in vehicle dynamic. Literature [26] also points out that compared with the number of degrees of freedom of vehicles, the overall accuracy of vehicle models is more significantly affected by the tire model. Therefore, it is necessary to establish an accurate tyre model to describe tyre forces which directly affect the analysis results. In this study, the Magic Formula tyre model is adopted for dynamic analysis, and its mathematical expressions are as follows:

$$\begin{cases} y(x) = D\sin\{C\arctan[Bx - E(Bx - \arctan Bx)]\} \\ Y(X) = y(x) + S_V \\ x = X + S_H \end{cases} \tag{7}$$

where, $Y(X)$ represents the tyre force, X denotes the tyre slip ratio λ_i or wheel slip angle α_i, coefficients B, C, D and E are the stiffness factor, shape factor, peak factor and curvature factor respectively, and S_V and S_H represent the vertical shift and horizontal shift respectively.

The wheel slip ratio of Magic Formula tyre model is given by:

$$\lambda_i = \begin{cases} \dfrac{R\omega_i - V_{\mathrm{w}i}}{R\omega_i}, & R\omega_i \ge V_{\mathrm{w}i} \\ \dfrac{V_{\mathrm{w}i} - R\omega_i}{V_{\mathrm{w}i}}, & R\omega_i \le V_{\mathrm{w}i} \end{cases} \tag{8}$$

The velocities of each wheel center in the wheel heading direction are obtained as follows:

$$V_{\mathrm{w}1} = \left(v_x - \frac{d_f}{2}r\right)\cos\delta + \left(v_y + l_f r\right)\sin\delta \tag{9}$$

$$V_{\mathrm{w}2} = \left(v_x + \frac{d_f}{2}r\right)\cos\delta + \left(v_y + l_f r\right)\sin\delta \tag{10}$$

$$V_{w3} = v_x + \frac{d_r}{2}r \tag{11}$$

$$V_{w4} = v_x - \frac{d_r}{2}r \tag{12}$$

Apart from the tyre slip ratio, the calculation of the Magic Formula parameters also requires the wheel slip angle which is defined as the angle between the wheel heading direction and the velocity vector of the wheel center. The wheel slip angle for each tire is expressed as:

$$\alpha_1 = arctan\frac{v_y + l_f r}{v_x - \frac{d_f}{2}r} - \delta - C_{\delta f}\emptyset \tag{13}$$

$$\alpha_2 = arctan\frac{v_y + l_f r}{v_x + \frac{d_f}{2}r} - \delta - C_{\delta f}\emptyset \tag{14}$$

$$\alpha_3 = arctan\frac{v_y - l_r r}{v_x + \frac{d_r}{2}r} - C_{\delta r}\emptyset \tag{15}$$

$$\alpha_4 = arctan\frac{v_y - l_r r}{v_x - \frac{d_r}{2}r} - C_{\delta r}\emptyset \tag{16}$$

where $C_{\delta f}$ and $C_{\delta r}$ represent the front and rear roll steer coefficients, respectively.

In the MF tyre model, the tyre load affects the scale of the peak factor D. The normal reaction forces for each wheel considering both longitudinal and lateral load transfers are written as follows:

$$F_{z1} = \frac{1}{2l}\left(mgl_r - h\sum F_x\right) - \frac{1}{d_f}\left(K_{\emptyset f}\emptyset + C_{\emptyset f}p + h_f\sum F_{yf}\right) \tag{17}$$

$$F_{z2} = \frac{1}{2l}\left(mgl_r - h\sum F_x\right) + \frac{1}{d_f}\left(K_{\emptyset f}\emptyset + C_{\emptyset f}p + h_f\sum F_{yf}\right) \tag{18}$$

$$F_{z3} = \frac{1}{2l}\left(mgl_f + h\sum F_x\right) + \frac{1}{d_r}\left(K_{\emptyset r}\emptyset + C_{\emptyset r}p + h_r\sum F_{yr}\right) \tag{19}$$

$$F_{z4} = \frac{1}{2l}\left(mgl_f + h\sum F_x\right) - \frac{1}{d_r}\left(K_{\emptyset r}\emptyset + C_{\emptyset r}p + h_r\sum F_{yr}\right) \tag{20}$$

where h_f and h_r denote the front and rear roll center height respectively.

D. NUMERICAL MODELING OF IN-WHEEL MOTOR

The vehicle model established in this paper is equipped with a in-wheel motor, whose performance parameters are shown in table 2. According to the characteristics of the motor, the efficiency of the motor is different at each working point, so this paper builds a numerical model of motor efficiency considering the complexity and accuracy, which can been see clearly in Figure 2. Thus, the driving/braking efficiency of the motor can be obtained by looking up the table.

III. CONTROLLER DESIGN

The stability controller designed in this paper adopts hierarchical control structure, as shown in Figure 3. The upper controller calculates the corrective yaw moment and longitudinal force needed to control the vehicle to back to the stable state based on the deviation between the actual driving state and the expected state. According to the corrective yaw moment, the lower controller determines the target torque of each wheel, and then distribute it to each wheel by controlling the motor.

TABLE 2. Parameters of in-wheel motor.

Symbol	Quantity	Value
P_e	Nominal power	7 kw
P_{max}	Peak power	15 kw
T_e	Nominal torque	120 N·m
T_{max}	Peak torque	260 N·m
n_e	Nominal speed	550 r/min
n_{max}	Maximum speed	1200 r/min

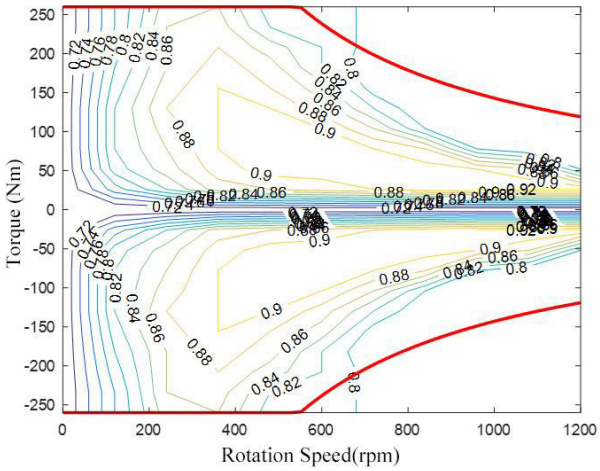

FIGURE 2. The motor efficiency mapping.

A. THE UPPER CONTROLLER

The vehicle system has nonlinear, time-varying and uncertain characteristics during high-speed steering of vehicle, especially for a FWIDEV. And as a typical nonlinear control method, sliding mode control (SMC) is adopted in this paper to solve the control problem of nonlinear systems.

The variables to be controlled in this study are the yaw rate$r$ and the sideslip angle β. Form a 2-DOF vehicle model [30], we can obtain the steady-state yaw rate response.

$$r_d = \frac{v_{xd}}{l(1+Kv_{xd}^2)}\delta \tag{21}$$

Combining the (21) with the variable steering ratio steering system in the 8-DOF model, the desired yaw rate can be obtained.

$$r_d = \frac{v_{xd}}{l(1+Kv_{xd}^2)}\frac{\theta_w}{j_v} = \frac{v_{xd}}{l(1+Kv_{xd}^2)}\frac{j\delta}{j_v} \tag{22}$$

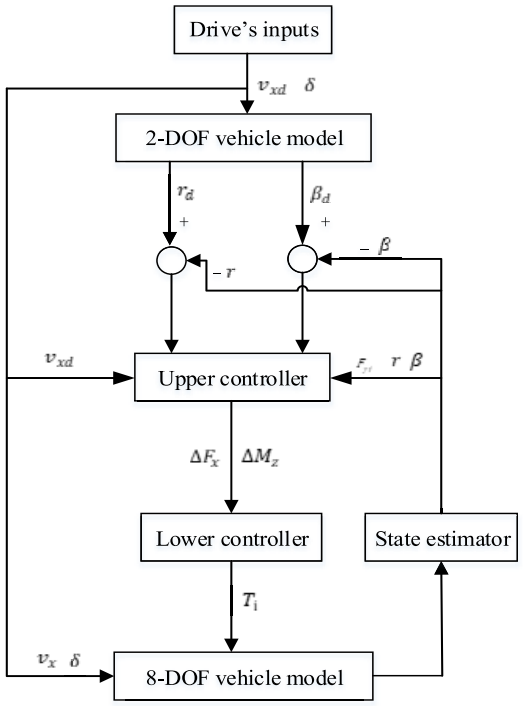

FIGURE 3. Schematic of the hierarchical control structure.

where, v_{xd} represents the ideal vehicle longitudinal speed, θ_w is the steering wheel angle. $\theta_w = j\delta$, j denotes the fixed steering ratio and its value is 15, j_v represents the variable steering ratio. K is the stability factor.

Considering the limitation of the adhesion conditions, the yaw rate r has the following relationship with the road surface adhesion coefficient and the vehicle speed.

$$|r| \leq 0.85\frac{\mu g}{v_{xd}} \tag{23}$$

Combining (22) and (23), we can obtain the desired yaw rate of the vehicle.

$$r_d = min\left(\left|\frac{v}{l\left(1+Kv_{xd}^2\right)}\frac{j\delta}{j_v}\right|, \left|0.85\frac{\mu g}{v_{xd}}\right|\right)\text{sgn}\,(\delta) \tag{24}$$

In order to ensure that the yaw rate transient response does not appear large oscillation or overshoot, the desired value in (24) is required for filtering. And the desired yaw rate is calculated at last.

$$r_d = min\left(\left|\frac{v}{l\left(1+Kv_{xd}^2\right)}\frac{j\delta}{j_v}\right|, \left|0.85\frac{\mu g}{v_{xd}}\right|\right) \times\text{sgn}\,(\delta)\frac{900}{s_t^2+48s_t+900} \tag{25}$$

where, s_t and μ represent the Laplacian and road adhesion coefficient respectively.

Referring to the related literature [31], [32], the value of the ideal sideslip angle is 0. And it is also limited by the road adhesion conditions

$$\beta \leq arctan\,(0.02\mu g) \tag{26}$$

The following optimized switching function is adopted [30].

$$s = \frac{\rho}{|\Delta r|_{max}}|r - r_d| + \frac{1-\rho}{|\Delta\beta|_{max}}|\beta - \beta_d| \tag{27}$$

where $|\Delta r|_{\max}$ and $|\Delta\beta|_{\max}$ are the maximum tolerable error of each control variable, and the range of weighting factor ρ is [0, 1].

Deriving (27) and combining the yaw motion equation (3) of the vehicle, and using the exponential approach law shown in (28) to obtain the required yaw moment of the vehicle ΔM_z.

$$\dot{s} = -\varepsilon\text{sgn}\,(s) - k_d s,\ \varepsilon > 0, k_d > 0 \tag{28}$$

$$\Delta M_z = I_z\left\{\begin{array}{l}\frac{|\Delta r|_{max}}{\rho}\left[-\varepsilon\text{sgn}\,((r-r_d)\,s) - k_2 s\text{sgn}\,(r-r_d)\right] \\ +\dot{r}_d - \frac{1-\rho}{\rho}\frac{|\Delta r|_{max}}{|\Delta\beta|_{max}}\dot{\beta}\text{sgn}\,((r-r^*)\,\beta)\end{array}\right\} - F_Y \tag{29}$$

where ε and k_d are the boundary layer thicknesses. Note that to reduce the chattering effects of the sign function, the saturation function 'sat' is adopted instead.

Since the vehicle has various types of resistance during running, it is necessary to control its longitudinal driving force to follow the desired vehicle speed. This paper will use SMC to realize the longitudinal driving force control of the vehicle. And the switching function is:

$$s_v = v_{xd} - v_x \tag{30}$$

Let ΔF_x denotes the longitudinal demand force, and derive the (30) and combine the longitudinal motion equation (1) of the vehicle body, and adopt the exponential approach law shown in (29) to obtain the longitudinal demand force of the vehicle:

$$\Delta F_x = m\left(\dot{v}_{xd} + v_y + \varepsilon sgn\,(s) + k_d s\right) + F_{y1}\sin\delta + F_{y2}\sin\delta + F_w + F_f m_s h_s p r \tag{31}$$

where v_{xd} represents the desired vehicle speed, v_x is the actual vehicle speed, and ε and k_d are controller design parameters.

B. THE LOWER CONTROLLER

There are several ways to distribute wheel torque under the premise of meeting control requirements and actuator limitations. Therefore, it is necessary to study the influence of different wheel torque distribution forms on vehicle stability and economy, and obtain the optimal distribution method of wheel torque under different working conditions.

There is a relationship expressed by (32) between the upper layer demand and the lower wheel torque distribution in vehicle stability control.

$$A_u x = b_u \tag{32}$$

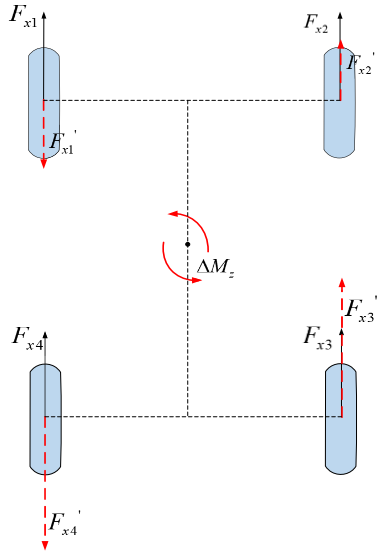

FIGURE 4. Schematic of diagram of wheel torque distribution between front and rear axles.

where, $x = \left[T_1\ T_2\ T_3\ T_4\right]^T$, $b_u = \left[\Delta F_x\ \Delta M_z\right]^T$, T_i represents the torque of each wheel, and $d = d_f = d_r$.

$$A_u = \frac{1}{R}\begin{bmatrix} \cos\delta & \cos\delta & 1 & 1 \\ -\frac{d}{2}\cos\delta + l_f\sin\delta & \frac{d}{2}\cos\delta + l_f\sin\delta & \frac{d}{2} & -\frac{d}{2} \end{bmatrix}$$

1) ANALYSIS OF THE INFLUENCE OF DESIRED YAW MOMENT DISTRIBUTION ON DIFFERENT WHEELS ON VEHICLE PERFORMANCE

a: DIFFERENT FRONT-TO-REAR WHEEL TORQUE DISTRIBUTIONS

According to the mathematical relation (33), the desired yaw moment is converted into the additional wheel torque ΔT. Study the effects of different torque distribution ratios on vehicle stability and economy under the condition of single lane change manoeuvre at 40 km/h. Take the direction of the required yaw moment as counterclockwise for example. In order not to affect the longitudinal speed of the vehicle, make the additional torques of the right and left coaxial wheels equal and opposite which can been see in Fig. 4.

$$\Delta T = \frac{2\Delta M_z}{d}R \tag{33}$$

Let 'a' be the ratio of the front axle torque to the total demand torque. Simulate and compare the vehicle yaw rate and the trajectory corresponding to different 'a' values, and obtain the results shown in Fig.5.

As can be seen in Fig.5, when the value of a is 0.5 (note: the closer the value is to the ratio of the front and rear wheelbases), the yaw rate and the trajectory of the vehicle are best for tracking the ideal values. And the worst results are achieved when the front or rear axle alone assumed all the required torque.

The simulation shows the economic performance of the vehicle (characterized by the motor comprehensive efficiency (34)).

$$J_e = \frac{T_1n_1 + T_2n_2 + T_3n_3 + T_4n_4}{\frac{T_1}{\eta_1}n_1 + \frac{T_2}{\eta_2}n_2 + \frac{T_3}{\eta_3}n_3 + \frac{T_4}{\eta_4}n_4} \tag{34}$$

The simulation results show that when the vehicle is turning (0.5-2.5 seconds), the economic performance is best when the proportional coefficient a is equal to 0.5, and the economic performance of a ratio equal to 0.25 or 0.75 is second. It means that when the value of the proportional coefficient a is closer to the ratio of the front and rear wheelbase of the vehicle, the vehicle is in a very stable state, and the economy is optimal in the steering process.

b: DIFFERENT TORQUE DISTRIBUTION ON THE COAXIAL LEFT AND RIGHT WHEELS

The front and rear axles each bear half of the required yaw moment, and compare the effects of the left and right wheels on the stability and economy of the vehicle when the ΔT is distributed in different ways.

In addition to the variable distribution of the torque distribution between the left and right wheels, there are various combinations between the torque directions. So this paper proposes a method to screen the possible left and right wheel torque distribution forms. Considering that the vehicle speed is not affected, the sum of the additional driving forces of the four wheels needs to be zero.

$$F_{x1}^{'} + F_{x2}^{'} + F_{x3}^{'} + F_{x4}^{'} = 0 \tag{35}$$

where, $F_{xi}^{'}$ represents the longitudinal force of each wheel required to satisfy the desired yaw moment.

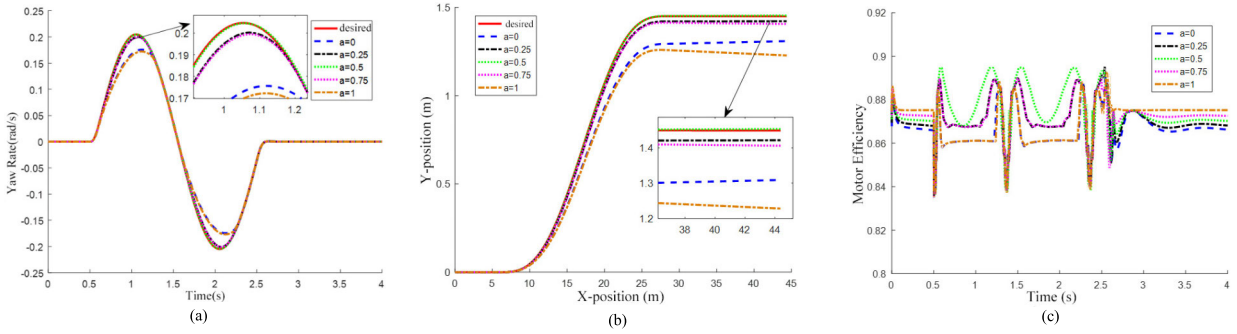

FIGURE 5. Vehicle yaw rate (a), driving trajectory (b) and motor comprehensive efficiency map (c) corresponding to different 'a' values.

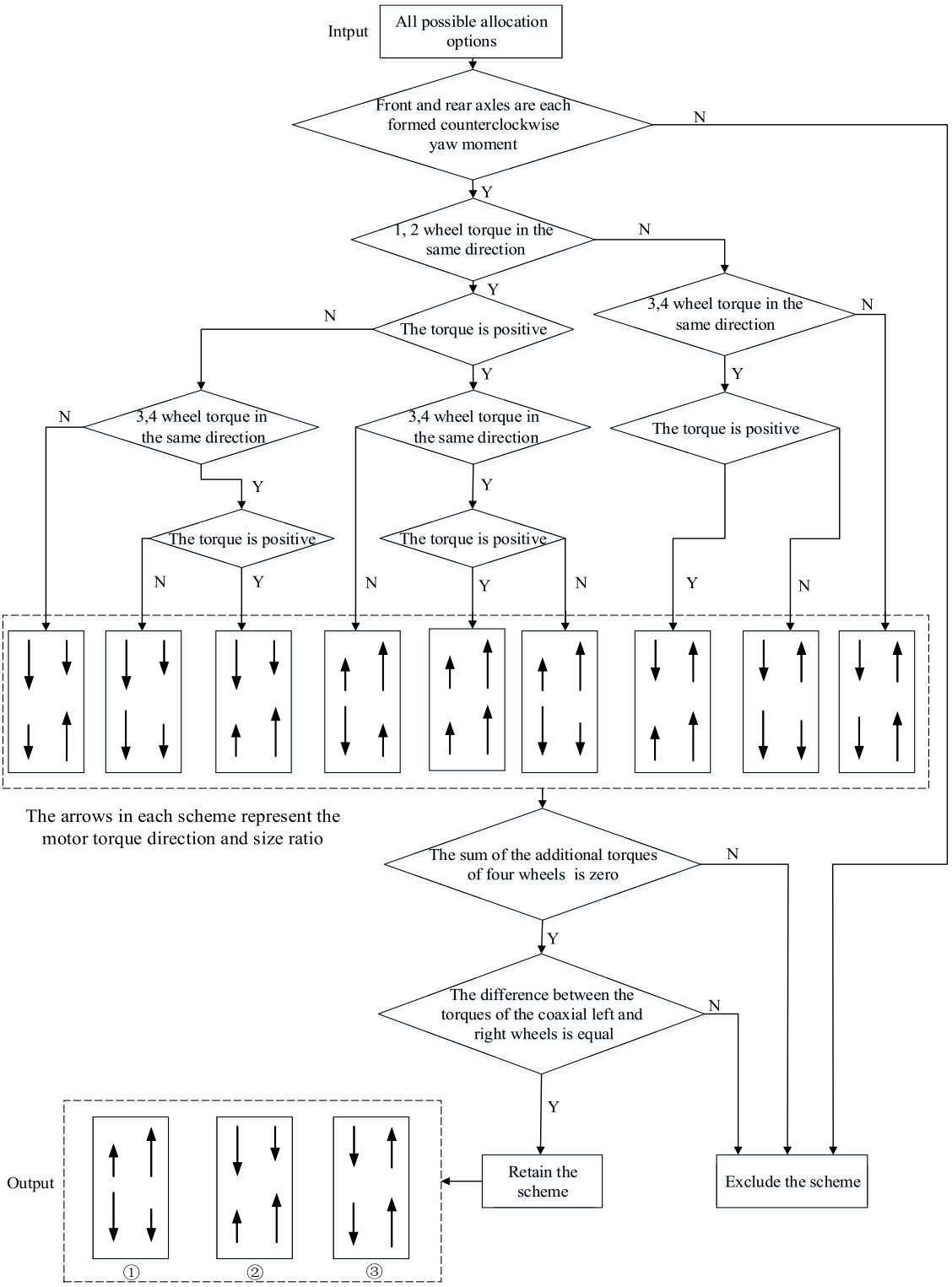

FIGURE 6. Left and right wheel torque distribution scheme selection flow chart.

In addition to meeting the requirements of equation (36), it is also required that the yaw moments formed by the front and rear axles are counterclockwise and equal. According to the above requirements, formulate a flow chart for the selection of the distribution plan. According to the flow shown in Fig.6, the schemes with the numbers ①, ②, and ③ satisfying all the requirements are finally obtained.

Definition b is the ratio of the torque on the left wheel to the total torque assumed by the axle. First, the solution ① is analyzed to compare the effects of different distribution ratios

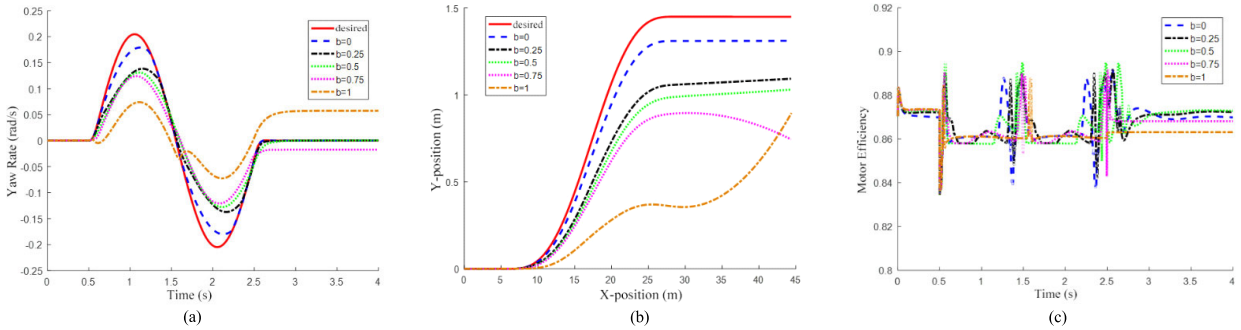

FIGURE 7. Vehicle yaw rate (a), driving trajectory (b) and overall efficiency of the motor (c) in option of option ①.

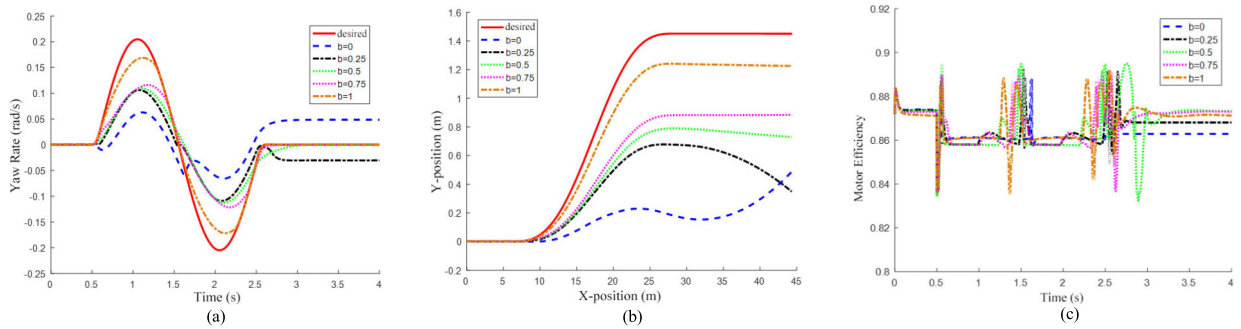

FIGURE 8. Vehicle yaw rate (a), driving trajectory (b) and overall efficiency of the motor (c) in option of option ②.

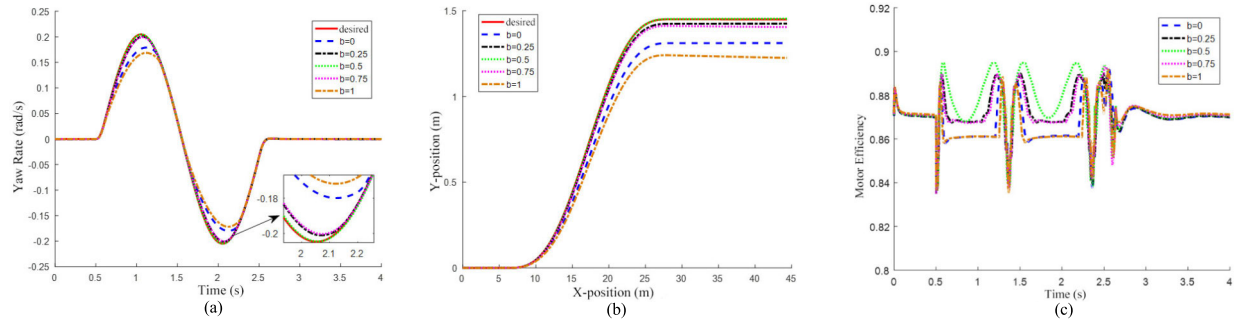

FIGURE 9. Vehicle yaw rate (a), driving trajectory (b) and overall efficiency of the motor (c) in option of option ③.

b on vehicle stability and economy, and the results shown in Fig.7 are obtained.

As can be seen from Fig.7, the yaw rate and the trajectory of the left and right wheels cannot track the ideal value well regardless of the torque distribution ratio of the left and right wheels. And when b>0.5, the torque direction formed by the wheel is clockwise, which is opposite to the desired torque direction, making the control effect worse.

Secondly, the effect of different distribution ratios between the left and right wheels on the vehicle performance in the case of option ② is studied, and the results shown in Fig.8 are obtained.

Comparing the simulation results of schemes ① and ②, we can find that the impact of the two on stability and economy is the same. The reason for this phenomenon is that the torque distribution methods of the two are essentially the same. The two schemes can be transformed from each other by different b values. This is illustrated by the fact that the stability and economic performance of the vehicle when b is 0 in Scheme ① is exactly the same as that when b is 1 in Option 2.

Finally, the third scheme is analyzed to obtain the results shown in Fig.9.

Figure 9 shows that the stability control effect is best when b equals 0.5, that is, the two coaxial wheels distribute the required yaw moment in opposite directions. And when a single wheel (b = 0 and b = 1) generates all the required yaw moments, the control effect is the worst, which means that the stability control of the vehicle is significantly affected by the position of the centroid. Meanwhile, it can be seen from

figure 13 that the economic performance during the steering of the vehicle is best when b is equal to 0.5.

Based on the analysis results of the above three schemes, it is known that when the scheme ③ is used and the torque is distributed by the front and rear axles proportional to the centroid position, the stability and economic performance of the vehicle when steering are the best. And the corresponding wheel torques are as follows:

$$T_1 = \left(0.25\Delta F_x - \frac{\Delta M_z}{2d_f}\right) R \tag{36}$$

$$T_2 = \left(0.25\Delta F_x + \frac{\Delta M_z}{2d_f}\right) R \tag{37}$$

$$T_3 = \left(0.25\Delta F_x + \frac{\Delta M_z}{2d_r}\right) R \tag{38}$$

$$T_4 = \left(0.25\Delta F_x - \frac{\Delta M_z}{2d_r}\right) R \tag{39}$$

2) WHEEL TORQUE OPTIMAL DISTRIBUTION CONTROL STRATEGY

The above studies only consider the torque distribution during the steering process of the vehicle. In order to comprehensively improve the economic performance of the vehicle, a torque distribution strategy with the optimal overall motor efficiency as the objective function is constructed.

$$\begin{aligned} J_e &= \max\left\{T_d n / \left[\frac{\lambda_T T_d n}{\eta_f} + \frac{(1-\lambda_T) T_d n}{\eta_r}\right]\right\} \\ &= \max\left(\frac{\lambda_T}{\eta_f} + \frac{1-\lambda_T}{\eta_r}\right)^{-1} \end{aligned} \tag{40}$$

where,λ_T represents the front axle torque distribution coefficient, η_f and η_r represent the efficiency of the front and rear axle drive motors, respectively.

Constraints are as follows:

$$\begin{cases} 0 \le \lambda_T \le 0.5 \\ 0 \le 0.5\lambda_T T_d \le T_{\max} \\ 0 \le 0.5(1-\lambda_T) T_d \le T_{\max} \end{cases} \tag{41}$$

Using the motor efficiency characteristic map, the front axle distribution coefficient can be solved as shown in Fig.10.

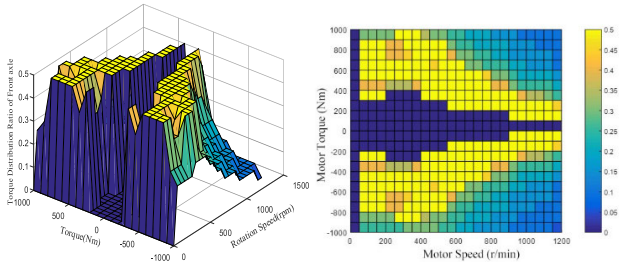

FIGURE 10. Front axle torque distribution coefficient.

According to the above research, in order to improve the economy while ensuring the stability of the vehicle, the optimal torque distribution control strategy for the vehicle under full working conditions is established., that is, the torque distribution is performed with the highest motor efficiency as the objective function when the vehicle goes straight, and the formula (36) -(39) is used when the vehicle turns. The torque distribution scheme shown is shown in Fig.11.

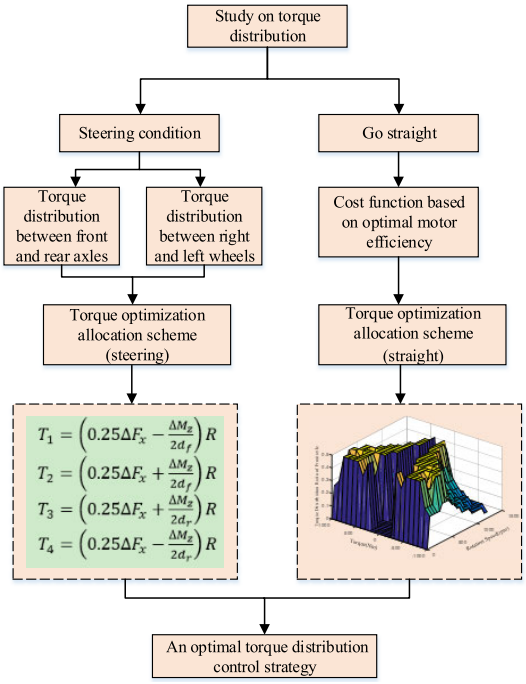

FIGURE 11. Block diagram of optimal torque distribution control strategy.

IV. SIMULATION RESULTS

The purpose of this paper is to improve the economy while ensuring the stability of the vehicle. In order to verify the effectiveness of the control strategy and test its impact on vehicle stability, the comparative simulation results of three different methods are presented. They are the proposed control strategy, the conventional stability control strategy and the passive system which constantly sends identical torque commands to the motors. In the following, for brevity, the three systems are referred to as the ''proposed method'', ''conventional method'' and ''uncontrolled'', respectively.

A. THE CONVENTIONAL STABILITY CONTROL STRATEGY

The conventional method means that the minimum surface adhesion consumption rate is the objective function to optimize the distribution of wheel torque expressed in (42).

$$\min J = \sum_{i=1}^{i=4} \frac{F_{xi}^2 + F_{yi}^2}{(\mu_i F_{zi})^2} \tag{42}$$

Standardizing the objective function:

$$\min_{uc} J = u_c^{\mathrm{T}} W_u u_c \tag{43}$$

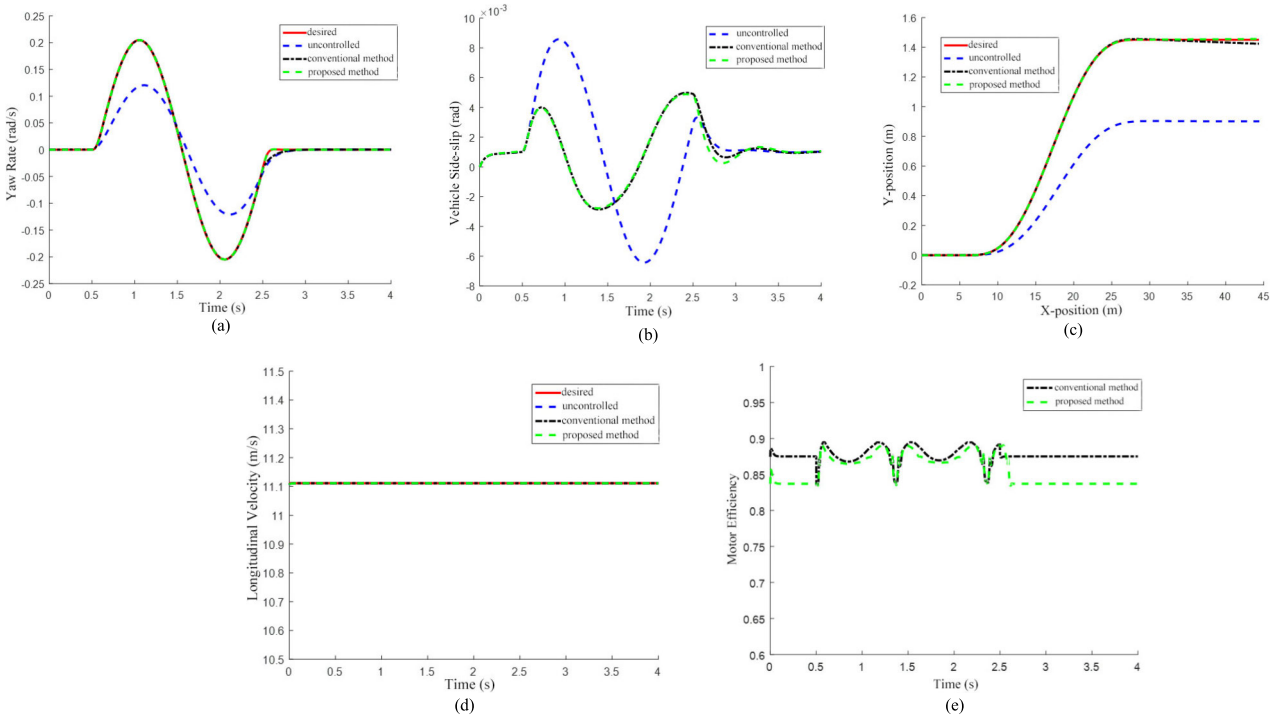

FIGURE 12. Simulation results for vehicle at ($\mu = 0.8, v = 40$km/h). (a) Yaw rate. (b) Side slip angle. (c) Track. (d) Speed. (e) Motor efficiency.

The constraints are as follows:

$$\begin{cases} B_c u_c = v_c \\ u_{cmin} \le u_c \le u_{cmax} \end{cases} \tag{44}$$

where, W_u represents the weighting coefficient of the control variable u_c. Ignore the lateral force F_{yi} in (42), then $W_u = diag\left(\frac{1}{(\mu_i F_{zi})^2}\right)$, $u_c = \left[F_{x1}\ F_{x2}\ F_{x3}\ F_{x4}\right]^{\mathrm{T}}$, $v_c = \left[\Delta F_x\ \Delta M_z\right]^T$,

$$B_c = \begin{bmatrix} \cos\delta & \cos\delta & 1 & 1 \\ -\frac{d}{2}\cos\delta + l_f \sin\delta & \frac{d}{2}\cos\delta + l_f \sin\delta & \frac{d}{2} & -\frac{d}{2} \end{bmatrix}$$

Substitute $B_c u_c = v_c$ with $\min \|\mathrm{B}_c u_c - v_c\|_2$, and the sequence least squares programming problem is transformed into a weighted least squares method by introducing a weight coefficient γ.

$$u_c = \underset{u_{cmin} \le u_c \le u_{cmax}}{\operatorname{argmin}} \left(\|\mathrm{W}_u u_c\|_2^2 + \gamma \|\mathrm{W}_v (B_c u_c - v_c)\|_2^2 \right) \tag{45}$$

where, W_v is the weight matrix to define the priority of each generalized control input. And the optimisation problem can be solved using active set methods.

B. SINGLE LANE CHANGE MANOEUVRE TEST

1) HIGH ADHESION COEFFICIENT ROAD

For this manoeuvre, the vehicle drives on a dry road with $\mu = 0.8$ and the longitudinal speed is 40km/h. The simulation results of the stability and economy of the vehicle under different control strategies are shown in Figure 12.

It can be seen from Fig.16 that in the aspect of stability control, both the proposed method and the conventional method can achieve better driving trajectory tracking effect, and the corresponding vehicle speeds can better follow the ideal value under the two control strategies that can meet the driving requirements. However, as for energy economy, the maximum and average values of the overall efficiency of the motor are improved under the comprehensive control strategy proposed in this paper, and the average value of the overall efficiency of the motor is increased by 2.44%. At the same time, the motor efficiency curve is more stable, and the standard deviation is 51.49% lower than the stability control strategy, which can reduce the motor torque ripple (Table 3).

TABLE 3. Motor comprehensive efficiency data statistics.

Motor efficiency	Control strategy	
	Conventional method	Proposed method
Maximum	0.8912	0.8949(↑0.42%)
Average	0.8563	0.8772(↑2.44%)
Standard variance	0.0202	0.0098(↓51.49%)

2) LOW ADHESION COEFFICIENT ROAD

For this manoeuvre, the vehicle drives on a slippery road with $\mu = 0.3$ and the longitudinal speed is 40km/h. The simulation results of the stability and economy of the vehicle under different control strategies are shown in Figure 13.

Fig.13 shows that under the road with low adhesion coefficient, the conventional method and the integrated control

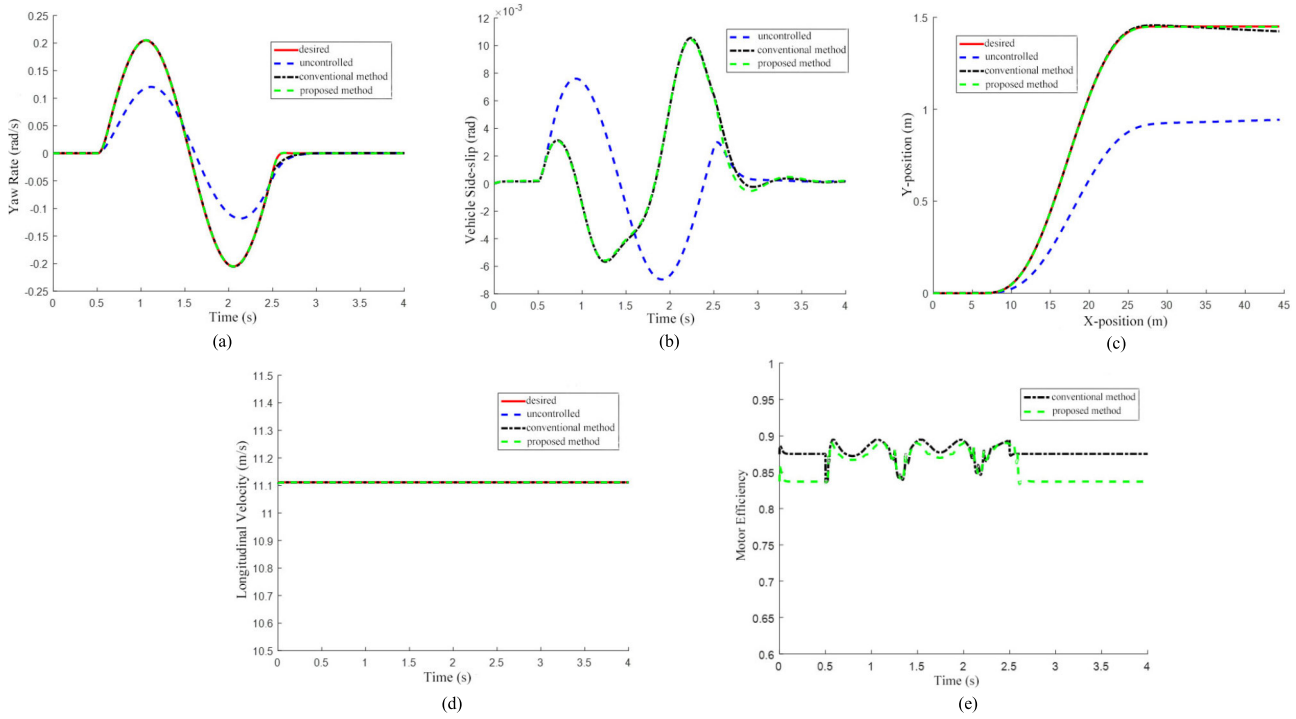

FIGURE 13. Simulation results for vehicle at ($\mu = 0.4, v = 40$km/h). (a) Yaw rate. (b) Side slip angle. (c) Track. (d) Speed. (e) Motor efficiency.

strategy proposed in this paper have similar performance in vehicle stability. comparing the motor comprehensive efficiency of the two control strategies, the overall economic performance of the vehicle controlled by proposed method is better than that of the conventional method, and the superiority is more obvious when the vehicle goes straight. Table 4 shows the details.

TABLE 4. Motor comprehensive efficiency data statistics.

Motor efficiency	Control strategy	
	Conventional method	Proposed method
Maximum	0.8909	0.8949(↑0.45%)
Average	0.8568	0.8775(↑2.42%)
Standard variance	0.0210	0.0101(↓51.9%)

The above simulation results show that the integrated control strategy proposed in this paper can effectively improve the energy economy in the control process under the premise of ensuring vehicle stability.

V. CONCLUSION

In this paper, the influence of different wheel torque distribution forms on vehicle stability and economy during the steering process is analyzed in depth, and then the wheel torque optimization distribution scheme during steering is proposed. A torque distribution scheme with the optimal motor efficiency as the objective function is constructed to improve the economy when the vehicle goes straight. On this basis, the optimal wheel torque distribution control strategy for the vehicle under full working conditions is proposed, and the effectiveness of the proposed control strategy is verified under single lane change manoeuvre.

The simulation results illustrate that compared with the conventional stability control strategy, the wheel torque optimization distribution control strategy proposed in this paper has the same stability control performance, but it performs better in terms of energy economy. That means it can reduce the energy consumption while ensuring vehicle stability.

REFERENCES

[1] C. Fu, R. Hoseinnezhad, A. Bab-Hadiashar, and R. N. Jazar, "Direct yaw moment control for electric and hybrid vehicles with independent motors," *Int. J. Vehicle Des.*, vol. 69, nos. 1-4, pp. 1–24, 2015.
[2] Y. Chen, J. K. Hedrick, and K. Guo, "A novel direct yaw moment controller for in-wheel motor electric vehicles," *Vehicle Syst. Dyn.*, vol. 51, no. 6, pp. 925–942, 2013.
[3] S. Li, D. Zhao, L. Zhang, and Y. Tian, "Lateral stability control system based on cooperative torque distribution for a four in-wheel motor drive electric vehicle," in *Proc. 36th Chin. Control Conf.*, Jul. 2017, pp. 1119–1123.
[4] T. Mi, C. Li, C. Hu, J. Wang, and R. Wang, "Robust H∞ output-feedback yaw control for in-wheel motor driven electric vehicles with differential steering," *Neurocomputing*, vol. 3, pp. 676–684, Jan. 2015.
[5] P. Oke, S. K. Nguang, and J. Wen, "H∞ dynamic output feedback control for independently driven four-wheel electric vehicles with differential speed steering," in *Proc. IEEE Int. Conf. Inf. Automat.*, Aug. 2017, pp. 567–572.
[6] G. Xuwei and S. Tao, "Study on algorithm of stability control based on 4-wheel-steering vehicle," *Electron. Sci. Tech.*, vol. 30, no. 8, pp. 48–55, 2017.
[7] G. Yin, H. Wu, N. Zhang, and J. Chen, "H_∞ robust controller design for 4WS-4WD vehicle based on LMI," *J. Southeast Univ. (Natural Sci. Ed.)*, vol. 46, no. 6, pp. 1165–1171, Nov. 2016.

[8] X. Fan and Z. Zhao, "Vehicle dynamics modeling and electronic stability program/ active front steering sliding mode integrated control," *Asian J. Control*, to be published.
[9] W. Zhao, X. Qin, and C. Wang, "Yaw and lateral stability control for four-wheel steer-by-wire system," *IEEE/ASME Trans. Mechatronics*, vol. 23, no. 6, pp. 2628–2637, Dec. 2018.
[10] K. Nam, S. Oh, H. Fujimoto, and Y. Hori, "Design of adaptive sliding mode controller for robust yaw stabilization of in-wheel-motor-driven electric vehicles," *World Electr. Vehicle J.*, vol. 5, no. 2, pp. 588–597, 2012.
[11] S. Yim and K. Yi, "Design of active roll control system and integrated chassis control for hybrid 4WD vehicles," in *Proc. 14th Int. IEEE Conf. Intell. Transp. Syst.*, Oct. 2011, pp. 1193–1198.
[12] B. Lenzo, F. Bucchi, A. Sorniotti, and F. Frendo, "On the handling performance of a vehicle with different front-to-rear wheel torque distributions," *Vehicle Syst. Dyn.*, vol. 57, no. 11, pp. 1685–1704, Mar. 2018.
[13] J. Song, "Integrated control of brake pressure and rear-wheel steering to improve lateral stability with fuzzy logic," *Int. J. Automot. Technol.*, vol. 13, no. 4, pp. 563–570, Jun. 2012.
[14] H. Sun, H. Zhao, K. Huang, and S. Zhen, "A new approach for vehicle lateral velocity and yaw rate control with uncertainty," *Asian J. Control*, vol. 20, no. 1, pp. 216–227, Jan. 2018.
[15] J. Tian, Y. Q. Wang, and N. Chen, "Research on Vehicle stability based on DYC and AFS integrated controller," *Appl. Mech. Materials.*, vols. 278–280, pp. 1510–1515, Jan. 2013.
[16] S. Ding, L. Liu, and W. Zheng, "Sliding mode direct yaw-moment control design for in-wheel electric vehicles," *IEEE Trans. Ind. Electron.*, vol. 64, no. 8, pp. 6752–6762, Aug. 2017.
[17] C. Zhang, D. Zhang, and J. Wen, "Design of driving control strategy of torque distribution for two—Wheel independent drive electric vehicle," *IOP Conf. Ser. Earth Environ. Sci.*, vol. 113, no. 1, Feb. 2018, Art. no. 012082.
[18] Y. Hu, X.-Z. Zhang, and Y.-N. Wang, "Design of vehicle stability control of distributed-driven electric vehicle based on optimal torque allocation," in *Proc. 33rd Chin. Control Conf.*, Jul. 2014, pp. 195–200.
[19] D. Kim, S. Hwang, and H. Kim, "Vehicle stability enhancement of four-wheel-drive hybrid electric vehicle using rear motor control," *IEEE Trans. Veh. Technol.*, vol. 57, no. 2, pp. 727–735, Mar. 2008.
[20] L. Li, Y. Lu, R. Wang, and J. Chen, "A three-dimensional dynamics control framework of vehicle lateral stability and rollover prevention via active braking with MPC," *IEEE Trans. Ind. Electron.*, vol. 64, no. 4, pp. 3389–3401, Apr. 2017.
[21] R. Tchamna and I. Youn, "Yaw rate and side-slip control considering vehicle longitudinal dynamics," *Int. J. Automot. Technol.*, vol. 14, no. 1, pp. 53–61, Feb. 2013.
[22] N. Zhang, H. Li, X. Zhang, and X. Lu, "An optimal torque distribution for electric vehicle based on sliding mode observer," in *Proc. 36th Chin. Control Conf.*, Jul. 2017, pp. 9373–9378.
[23] D. Wu, Y. Li, J. Zhang, and D. Du, "Torque distribution of a four in-wheel motors electric vehicle based on a PMSM system model," *Proc. Inst. Mech. Eng., D, J. Automobile Eng.*, vol. 232, no. 13, pp. 1828–1845, 2018.
[24] J. Yamakawa and K. Watanabe, "A method of optimal wheel torque determination for independent wheel drive vehicles," *J. Terramech.*, vol. 43, no. 3, pp. 269–285, Jul. 2006.
[25] J. J. Eckert, L. C. de Alkmin e Silva, F. M. Santiciolli, E. dos Santos Costa, F. C. Corrêa, and F. G. Dedini, "Energy storage and control optimization for an electric vehicle," *Int. J. Energy Res.*, vol. 42, no. 11, pp. 3506–3523, Sep. 2018.
[26] X. Zhifeng, *Hnading Stability and energy Efficient Control for Distribution Drive Electric Vehicles*. Beijing, China: Beijing Institute of Technology, 2016.
[27] J. Hu, X. Niu, X. Jiang, and G. Zu, "Energy management strategy based on driving pattern recognition for a dual-motor battery electric vehicle," *Int. J. Energy Res.*, vol. 43, pp. 3346–3364, Jun. 2019.
[28] O. Mokhiamar and M. Abe, "How the four wheels should share forces in an optimum cooperative chassis control," *Control Eng. Pract.*, vol. 14, no. 3, pp. 295–304, Mar. 2006.
[29] W. Klier, G. Reimann, and W. Reinelt, "Concept and functionality of the active front steering system," SAE Tech. Paper 2004-21-0073, 2004.
[30] C. Fu, "Direct yaw moment control for electric vehicles with independent motors," Ph.D. dissertation Mech. Manuf. Eng., RMIT Univ. Melbourne VIC, Australia, 2014.
[31] B. Li, S. Rakheja, and Y. Feng, "Enhancement of vehicle stability through integration of direct yaw moment and active rear steering," *Proc. Inst. Mech. Eng., D, J. Automobile Eng.*, vol. 230, no. 6, pp. 830–840, 2016.
[32] A. Tota, B. Lenzo, Q. Lu, A. Sorniotti, P. Gruber, S. Fallah, and D. Smet, "On the experimental analysis of integral sliding modes for yaw rate and sideslip control of an electric vehicle with multiple motors," *Int. J. Automot. Technol.*, vol. 19, no. 5, pp. 811–823, Oct. 2018.

JIANJUN HU received the B.S., M.S., and Ph.D. degrees in automotive engineering from Chongqing University, Chongqing, China. His research interests include vehicle power transmission, hybrid electric vehicle control, and motor control used for electric vehicle.

JUNLONG TAO received the B.Eng. degree in automotive engineering from Fuzhou University, in 2017. He is currently pursuing the master's degree in automotive engineering with Chongqing University, China. His research interests include hybrid electric vehicle energy management strategy and vehicle handling stability control.

FENG XIAO received the B.S. degree from Nanchang University, Nanchang, Jiangxi, China, in 2018. He is currently pursuing the Ph.D. degree in vehicle engineering with Chongqing University. His research interests include motor control and stability control for vehicle chassis used in electric vehicle.

XIYUAN NIU received the M.S. degree in automotive engineering from Chongqing University, in 2019. She is currently a Chassis Engineer with the GAC Research and Development Center. Her research interests include hybrid electric vehicle energy management strategy and vehicle handling stability control.

CHUNYUN FU received the bachelor's degree from Chongqing University, China, in 2010, and the Ph.D. degree from RMIT University, Australia, in 2015. He is currently a Lecturer with the School of Automotive Engineering, Chongqing University. He has published over 20 articles in reputable journals and conference proceedings. His main research interests include autonomous vehicles and electric vehicles.